How to cite: *Angew. Chem. Int. Ed.* **2020**, *59*, 23239–23243
International Edition: doi.org/10.1002/anie.202010006
German Edition: doi.org/10.1002/ange.202010006

NMR Spectroscopy | Hot Paper

Efficient Encounter Complex Formation and Electron Transfer to Cytochrome *c* Peroxidase with an Additional, Distant Electrostatic Binding Site

*Antonella Di Savino, Johannes M. Foerster, Thijmen La Haye, Anneloes Blok, Monika Timmer, G. Matthias Ullmann, and Marcellus Ubbink**

Abstract: *Electrostatic interactions can strongly increase the efficiency of protein complex formation. The charge distribution in redox proteins is often optimized to steer a redox partner to the electron transfer active binding site. To test whether the optimized distribution is more important than the strength of the electrostatic interactions, an additional negative patch was introduced on the surface of cytochrome c peroxidase, away from the stereospecific binding site, and its effect on the encounter complex as well as the rate of complex formation was determined. Monte Carlo simulations and paramagnetic relaxation enhancement NMR experiments indicate that the partner, cytochrome c, interacts with the new patch. Unexpectedly, the rate of the active complex formation was not reduced, but rather slightly increased. The findings support the idea that for efficient protein complex formation the strength of the electrostatic interaction is more critical than an optimized charge distribution.*

Introduction

Electrostatic interactions are fundamental in protein-protein interactions and formation of protein complexes. Charge-charge interactions guide the recognition and binding between proteins and between a protein and a ligand.[1] Before forming the stereospecific, active complex, proteins associate into an intermediate state, the encounter complex, consisting of an ensemble of transient conformations, in which the proteins sample the surface of the partner.[2] The encounter complex is thought to reduce the dimensionality of the search for the binding site.[3] During this process electrostatic interactions contribute to pre-organization of the protein orientations in the encounter complex, reducing the surface area to be sampled and promoting the formation of stereospecific complex. The encounter complex formation is initially mostly driven by long-range electrostatic interactions. Upon closer approach of the two proteins, hydrophobic interactions also come into play, ultimately leading to the formation of the stereospecific complex.[4] The association rate constant, the measure for productive complex formation, can be four orders of magnitude lower than the diffusional collision rate constant in cases in which complex formation is not optimized, indicating that most encounters are non-productive and partners dissociate before reaching the stereospecific complex. Such encounters are called futile.[5] On the other hand, association rate constants approach the collision rate constant for some complexes, which is thought to be caused by strong electrostatic pre-organization of the encounter complexes, with the charge interactions guiding the partners to the correct orientation for binding.[1a] For such complexes, charge distribution over the surfaces of the proteins is expected to be optimized by evolution. The complex formed by cytochrome P450cam and putidaredoxin was previously studied to understand the function of the different encounter complexes formed by the two proteins. The data suggest that the encounter complexes located in a region with an electrostatically favorable pathway to the stereospecific binding site represent productive encounter states. On the contrary, encounter complexes located far from the binding site and in absence of a favorable charged path that extends to the binding site consist of futile interactions.[6] The encounter complex is therefore a key stage in the formation of a protein complex and mutations that affect the encounter complex have consequences for the stereospecific protein complex. Previous studies by Harel et al.[5a] on the interactions between TEM1-β-lactamase (TEM1) and its inhibitor, β-lactamase-inhibitor protein (BLIP), showed that it is difficult to define a correlation between the energy of the interaction, the surface area searched by the encounter complex and the association rate between two proteins. Recently, it was shown that futile encounter complexes could have a role in regulation of enzyme activity forming competitive encounter complexes.[7] Interestingly, charge mutations on the protein surface far from the active site can either enhance complex formation by creating new productive encounter complexes, or decrease it by breaking diffu-

[*] A. Di Savino, T. La Haye, A. Blok, M. Timmer, M. Ubbink
Leiden University, Institute of Chemistry
Einsteinweg 55, 2333 CC Leiden (Netherlands)
E-mail: m.ubbink@chem.leidenuniv.nl
J. M. Foerster, G. M. Ullmann
University of Bayreuth, Computational Biochemistry
Universitätsstraße 30, NW I, 95447 Bayreuth (Germany)
T. La Haye
Present address: University of Delft, TNW Applied Sciences
Van der Maasweg 9, 2629 HZ Delft (The Netherlands)
Supporting information and the ORCID identification number(s) for the author(s) of this article can be found under: https://doi.org/10.1002/anie.202010006.

© 2020 The Authors. Published by Wiley-VCH GmbH. This is an open access article under the terms of the Creative Commons Attribution Non-Commercial NoDerivs License, which permits use and distribution in any medium, provided the original work is properly cited, the use is non-commercial, and no modifications or adaptations are made.

sional pathways over the surface that would lead to the formation of the stereospecific complex.[8] We wondered how critical such a charge distribution is for fast complex formation in an optimized complex, as compared to the total strength of the electrostatic interactions. Good complexes to study this question are those formed by electron transfer (ET) proteins, as these are highly transient, that is, have a high association and dissociation rate constants, and the fraction of the encounter complex is high. The reason for these features is related to the biological function. Transfer of electrons in redox chains, such as found in photosynthesis and respiration, can be rate-limiting for the entire process and, thus, complex formation must be efficient. One of the best characterized ET complexes is the one formed by cytochrome *c* peroxidase (CcP) and cytochrome *c* (Cc) from baker's yeast (*Saccharomyces cerevisiae*). The formation of the encounter complex is driven by electrostatic interactions between positive charges on Cc and negative charges on CcP.[9] The encounter state and the stereospecific complex represent 30% and 70% of the complex, respectively.[10] Due to the electrostatic pre-organization, the area sampled by Cc was estimated to be merely 15% of the CcP surface.[10b] The fraction of encounter complex was found to be affected by mutations in the binding site, with the fraction of the encounter complex ranging from 10% to 90% for different mutations.[11] CcP catalyzes the reduction of H_2O_2 to water using electrons donated by reduced Cc. The reaction proceeds through a complicated cycle, during which two molecules of Cc interact with CcP sequentially, each contributing one electron (Text S2). In line with other ET complexes, the ET rate is high ($>50\,000\ s^{-1}$),[12] the lifetime of the complex is short (0.1–1 ms),[13] the association rate constant very high (10^8–$10^9\ M^{-1}s^{-1}$ at 200 mM ionic strength)[14] and the affinity in the micromolar range ($K_D = 5\ \mu M$).[13] In a previous study by Erman and coworkers[15] several charge-reversal mutants of CcP were created to determine the impact of the charges on the surface of the protein on the association with Cc. The majority of these mutations, mainly the ones located in or around the binding site of Cc, significantly decreased the affinity between the two proteins. Interestingly, three of these mutations (D37K, E28K, and E209K) are slightly more distant from the binding site and two of them on the opposite side of the protein (D165K and D241K). Although it is possible that the mutation D241K could affect the stability of the protein, this study shows that the charged residues on the surface, also located far from the binding site, have a role in the association process of Cc and CcP.

To establish how important the optimization of the charge distribution on CcP is for achieving these ET specifications, we decided to change the charge distribution on the CcP surface by adding a new negative patch in addition to the existing one surrounding the binding site for Cc. The new patch interferes with the distribution of negative charge in native CcP that appears to be optimized for Cc honing into the stereospecific binding site. Thus, we expected that productive complex formation would be affected negatively, leading to more futile encounters. The interaction with this mutant CcP (CcP_B) was studied using Monte Carlo electrostatic calculations, paramagnetic relaxation enhancement (PRE) NMR spectroscopy and stopped-flow kinetic measurements to determine the association rate constant as a function of ionic strength. Both modelling and PRE-NMR demonstrate that the new negative patch is visited by Cc in the encounter state. Yet, to our surprise, the association rate is not reduced relative to the interaction with wild type CcP (CcP_A), and even appears to be enhanced slightly at moderate ionic strength. These observations indicate that the precise charge distribution around the binding site is less critical for complex formation than expected and the increased strength of the electrostatic interactions may compensate for a less optimal encounter complex.

Results and Discussion

Monte Carlo Simulations Show Cc to Interact with the Added Patch on CcP

To test how important the charge distribution of CcP is for binding and reduction by Cc, an additional negative patch was created on one side of the regular binding site for Cc, by changing four positive sidechains to negative ones (mutations K21E, K29E, K90E, and K97E), thus introducing a net charge change of −8 (Figure 1a,b). This construct, CcP_B, was characterized by Monte Carlo simulations, NMR spectroscopy and stopped-flow spectroscopy. Rigid-body Monte Carlo simulations, based only on electrostatic and steric interactions, were used to simulate the encounter complexes of Cc with CcP_A or CcP_B. Figure 1c shows CcP in ribbon representation and the ensemble of Cc centers-of-mass based on electrostatic interaction energies. The densest regions represent the most favorable Cc orientations. The interactions of Cc with CcP_A (cyan spheres) are predominantly found at the location of the stereospecific binding site, in accord with earlier calculations[9b,e,10b,17] According to the simulations, the mutations introduced on the CcP_B surface considerably affect the encounter complex, with Cc sampling the area with the added negative charges of CcP_B (magenta spheres) more frequently than the crystallographic binding site. Note that these calculations only consider electrostatic interactions. In the stereospecific complex additional favorable interactions are present, so the total interaction is not expected to shift as dramatically as follows from these calculations. Still, it is clear that these extra negative charges should have a significant effect on the distribution of Cc in the encounter state.

Affinity and Binding of Cc is Similar for CcP_A and CcP_B

NMR titration experiments of Cc and CcP_A and CcP_B (S.I. Text S1 and Figures S1, S2) show that the introduction of the additional charges has surprisingly little effect on the affinity and binding effects in the HSQC spectrum. It is noted that CSP are predominantly caused by the stereospecific complex and not by the encounter complex. In the latter, solvation is likely to be similar to that for free Cc and binding occurs in many orientations. Both factors contribute to

 © 2020 The Authors. Published by Wiley-VCH GmbH

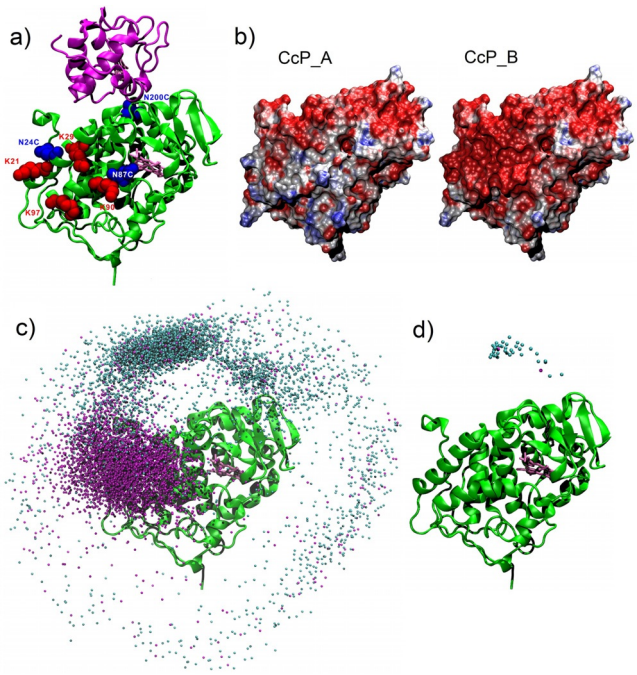

Figure 1. A new negative patch on CcP. a) Crystal structure of the stereospecific complex formed by Cc (magenta ribbons) and CcP (green ribbons) is shown (PDB 2PCC[9a]). The heme groups are shown in pink sticks, the residues that were mutated to introduce additional negative charges in CcP_B are in red space-filling representation and the residues mutated to cysteines for PRE experiments in blue space-fill. b) Electrostatic potential on the surface of CcP_A and CcP_B ranging from −5 (red) to 5 kcal/e° (blue) at an ionic strength of 120 mM. c) The structure of CcP (green ribbon) is surrounded by the centers of the mass of Cc in the ensemble of encounters of the complexes Cc:CcP_A (cyan) and Cc:CcP_B (magenta) as obtained from rigid body Monte Carlo simulations. d) The structure of CcP (green ribbon) is surrounded by the centers of the mass of Cc in the ensemble of encounters of the complexes Cc:CcP_A (cyan) and Cc:CcP_B (magenta) in which the edge-to-edge distance between Cc heme and the indole of the CcP compound I radical forming Trp (Trp-191) is less than 1.6 nm, as obtained from rigid body Monte Carlo simulations using the program MCMap.[24] CcP is in the same orientation in all panels. The pictures were produced with VMD.[16]

minimal perturbations of the chemical environment of the amide groups observed in the HSQC experiment. Desolvation and a well-defined orientation in the stereospecific complex are expected to cause most of the CSP.[18] So it appears that the additional charges do not cause a major shift in the equilibrium between encounter state and stereospecific complex, reported to be 30%:70%,[10] because that would have changed the overall size of the CSP.

PRE Experiments Demonstrate that Cc Interacts with the New Negative Patch

To establish whether Cc visits the new negative patch in the encounter state, we employed paramagnetic relaxation enhancement (PRE) NMR spectroscopy. PRE are very sensitive to minor states in which a nucleus is closer to the paramagnetic center than in the major state, because of the large relaxation effect of unpaired electrons and the steep distance dependence of the effect (r^{-6}).[19] To probe for such Cc interactions, two amino acids surrounding the new negative patch on CcP_B were individually mutated to cysteines (N87C and N24C, see Figure 1). These positions surround the new negative patch but are far from the regular Cc binding site. The mutations were also made in CcP_A. A third cysteine was introduced near the binding site of Cc (N200C) as a control. PRE data for this site have been reported before for the complex of CcP with WT Cc as well as several mutants.[11,20] The cysteine residues were used for the attachment of the small, stable spin label MTSL that causes PRE in a sphere of up to 2.5 nm. The spin labelled CcP_B was mixed with ^{15}N labelled Cc to record intermolecular PRE, from the CcP spin label on the Cc nuclei. The spin labels on the mutants N87C, N24C, and N200C of CcP_B induced large PRE in Cc (Figure 2). Analogous experiments on CcP_A mutant spin labelled at N87C and N24C showed much smaller PRE (Figure 2), whereas the effects for N200C were similar to those for CcP_B and those reported before.[10a] Thus, the large differences in PRE between CcP_A and CcP_B provide strong evidence that the new negative patch has become part of the encounter complex and is visited by Cc.

Binding at the New Negative Patch Yields Productive Encounters

The aim of this project was to determine whether the charges involved in formation of the encounter complex need to surround the binding site for the stereospecific complex to achieve optimal electron transfer. The NMR results show that the encounter complex has changed in CcP_B, extending the encounter complex away from the stereospecific binding site. To monitor whether the formation of productive, that is, electron transfer active, complexes is affected by the charges added to the surface of CcP_B, the association rate constant was determined by stopped-flow spectrometry, following early work of Miller et al.[14] In these experiments, CcP is first reacted with hydrogen peroxide to form the oxyferryl/Trp-radical species (compound I)[21] and then mixed rapidly with reduced Cc. The ensuing electron transfer from Cc^{II} to compound I, forming Cc^{III} and compound II,[22] is followed in time as a change in Cc absorption at 416 nm (see Text S2 and Figure S3). It can be shown that the observed second order rate constant is a lower limit of the association rate constant for productive complex formation, see Equation (3) in the Experimental Procedures in the Supplementary Information.[1a] In the present case, the observed rate constant (k_2) approaches the association rate constant (k_a) because the electron transfer rate (k_{et}) is much larger than the dissociation rate constant (k_{-a}). Association is strongly ionic strength dependent,[23] because of the favorable electrostatic interactions between CcP and Cc. The results are shown in Figure 3 and Table S1. Interestingly, they show that Cc forms a productive, reactive complex at least as effectively with CcP_B as with CcP_A. At moderate ionic strength the rate constants are even slightly higher, indicating a more favorable interaction. Given the fact that the rates for the Cc-CcP_A interaction at low ionic strength are over 10^9 $M^{-1}s^{-1}$, and thus

 © 2020 The Authors. Published by Wiley-VCH GmbH

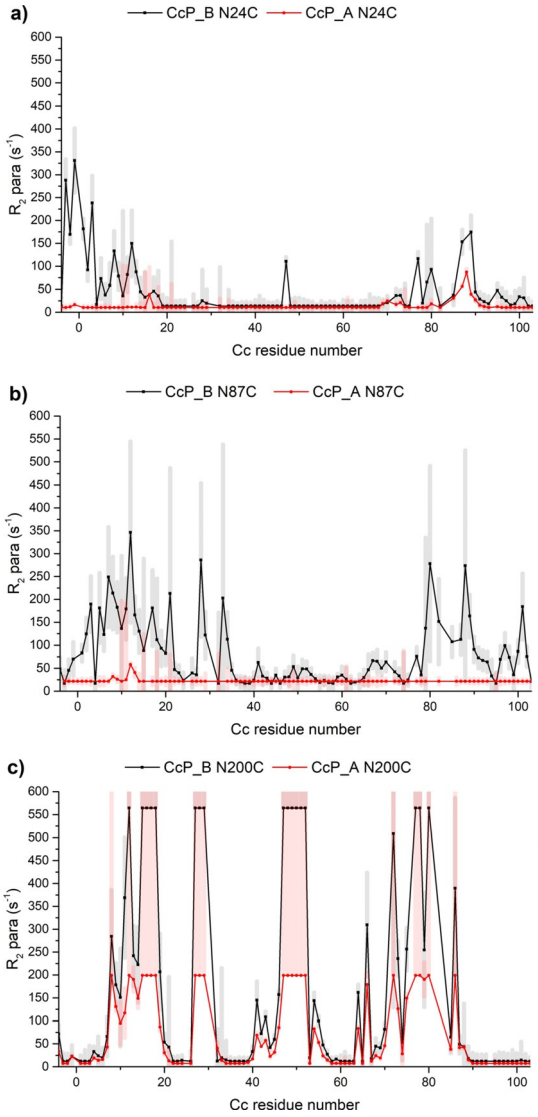

Figure 2. Probing new interactions with PRE NMR. The PRE on Cc in presence of CcP_A (in red) or CcP_B (in black), tagged with MTSL on a) N24C and b) N87C, both located around the negative patch introduced in CcP_B, and c) N200C close to the stereospecific binding site. The errors bars are indicated as shaded regions in red for Cc:CcP_A and in grey for Cc:CcP_B and represent the propagated 2 SD errors of the raw data. The upper and lower limit cut-offs for PRE differ between samples, depending on the fraction of CcP that was paramagnetic, as based on EPR measurements (see the Experimental Sections in the Supplementary Information for details).

close to the diffusion limit, it is remarkable that with CcP_B Cc achieves even faster association. To check whether this could be explained by possible ET from Cc bound to the new encounter site in addition of ET in the stereospecific complex the edge-to-edge distance between Cc heme and the indole of the CcP compound I radical forming Trp (Trp-191) was measured for all Cc orientations observed in the Monte Carlo simulation of CcP_B (Figure 1 d). All orientations of Cc in the new negative patch yield distances >1.6 nm, suggesting that the rate of ET would be negligibly slow from this site. Shorter distances are only found for Cc binding near the stereospecific complex. Thus, to achieve ET Cc that binds at the new patch

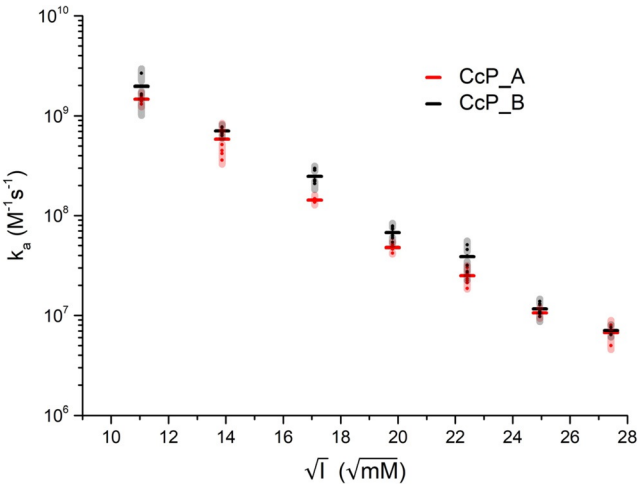

Figure 3. Association rate constants of Cc and CcP. The association rate constants (k_a) of the complexes Cc:CcP_A (red symbols) and Cc:CcP_B (black symbols) plotted as a function of the root of the ionic strength. The colored dots represent the k_a values obtained from fitting averages of 14 single measurements, while the bars represent the average of the dots. The errors in the rate constants are shown as shades and represent the standard deviation between the dots (see the Experimental Procedures section in the Supplementary Information for details).

needs to diffuse to the binding site of the stereospecific complex to form a productive complex. It is concluded, therefore, that the additional charges enhance the chance of the formation of the productive complex, even though the new charges are on the side of CcP, relative to the stereospecific binding site (Figure 1). This is consistent with the idea that encounter complexes close to the binding site consist of productive encounters because they promote the formation of the stereospecific complex.[6]

Conclusion

In summary, an additional negative patch was introduced on the surface of CcP, on a side respect to its stereospecific binding site for Cc (Figure 1). Both the Monte Carlo calculations and the PRE data indicate that Cc interacts with the new patch, yet this does not perturb the formation of the stereospecific complex. Earlier work demonstrated that the natural electrostatic patch of CcP optimally directs Cc to the site of stereospecific complex.[9a,b,e,10b,17] However, an optimized distribution of the charges around the stereospecific binding site is apparently not critical. Cc molecules that bind at the new negative patch can find their way to the stereospecific binding site before dissociation of the encounter complex. The new site thus produces productive rather than futile encounters.[1a,19a] CcP_B has a much larger negative charge compared to CcP_A. We conclude that the positive effect of the increased strength of the electrostatic interaction on the association rate outweighs the negative effect of a less optimized charge distribution.

 © 2020 The Authors. Published by Wiley-VCH GmbH

Acknowledgements

We thank Dr. Martina Huber and Enrico Zurlo for their valuable support in the EPR measurements, and Dr. B. I. Florea for the mass spectrometry analysis. This work was supported by the Netherlands Organisation for Scientific Research (NWO-CW grant 711.013.007 to MU), by the Deutsche Forschungsgemeinschaft (DFG grant SFB 1357 (TP C03) to GMU) and the study program "Biological Physics" of the Elite Network of Bavaria (J.M.F. and G.M.U.).

Conflict of interest

The authors declare no conflict of interest.

Keywords: electrostatic interactions · encounter complexes · NMR spectroscopy · paramagnetic relaxation enhancement · protein–protein interactions

[1] a) G. Schreiber, G. Haran, H. X. Zhou, *Chem. Rev.* **2009**, *109*, 839 – 860; b) M. Ubbink, *Biochem. Soc. Trans.* **2012**, *40*, 415 – 418; c) J. Yang, Y. F. Zeng, Y. F. Liu, M. Gao, S. Liu, Z. D. Su, Y. Q. Huang, *J. Biomol. Struct. Dyn.* **2020**, *38*, 4883 – 4894; d) H. X. Zhou, X. D. Pang, *Chem. Rev.* **2018**, *118*, 1691 – 1741; e) G. M. Clore, *Biophys. Chem.* **2014**, *186*, 3 – 12.

[2] J. Schilder, M. Ubbink, *Curr. Opin. Struct. Biol.* **2013**, *23*, 911 – 918.

[3] G. Adam, M. Delbrück in *Structural Chemistry and Molecular Biology* (Ed.: N. D. A. Rich), W. H. Freeman and Co., San Francisco, **1968**, p. 198.

[4] a) Y. C. Kim, C. Tang, G. M. Clore, G. Hummer, *Proc. Natl. Acad. Sci. USA* **2008**, *105*, 12855 – 12860; b) K. Van de Water, N. A. J. van Nuland, A. N. Volkov, *Chem. Sci.* **2014**, *5*, 4227 – 4236; c) S. Scanu, J. M. Foerster, G. M. Ullmann, M. Ubbink, *J. Am. Chem. Soc.* **2013**, *135*, 7681 – 7692; d) K. Sugase, H. J. Dyson, P. E. Wright, *Nature* **2007**, *447*, 1021-U1011; e) C. J. Camacho, Z. Weng, S. Vajda, C. DeLisi, *Biophys. J.* **1999**, *76*, 1166 – 1178; f) C. J. Camacho, S. R. Kimura, C. DeLisi, S. Vajda, *Biophys. J.* **2000**, *78*, 1094 – 1105; g) C. J. Camacho, S. Vajda, *Curr. Opin. Struct. Biol.* **2002**, *12*, 36 – 40; h) D. Rajamani, S. Thiel, S. Vajda, C. J. Camacho, *Proc. Natl. Acad. Sci. USA* **2004**, *101*, 11287 – 11292.

[5] a) M. Harel, A. Spaar, G. Schreiber, *Biophys. J.* **2009**, *96*, 4237 – 4248; b) N. L. Fawzi, M. Doucleff, J. Y. Suh, G. M. Clore, *Proc. Natl. Acad. Sci. USA* **2010**, *107*, 1379 – 1384.

[6] W. Andrałojć, Y. Hiruma, W. M. Liu, E. Ravera, M. Nojiri, G. Parigi, C. Luchinat, M. Ubbink, *Proc. Natl. Acad. Sci. USA* **2017**, *114*, E1840 – E1847.

[7] a) M. Strickland, S. Kale, M. P. Strub, C. D. Schwieters, J. Liu, A. Peterkofsky, N. Tjandra, *J. Mol. Biol.* **2019**, *431*, 2331 – 2342; b) S. Kale, M. Strickland, A. Peterkofsky, J. Liu, N. Tjandra, *Biophys. J.* **2019**, *117*, 1655 – 1665.

[8] S. Y. An, E.-H. Kim, J.-Y. Suh, *Structure* **2018**, *26*, 887 – 893.e882.

[9] a) H. Pelletier, J. Kraut, *Science* **1992**, *258*, 1748 – 1755; b) R. R. Gabdoulline, R. C. Wade, *J. Mol. Biol.* **2001**, *306*, 1139 – 1155; c) T. L. Poulos, S. T. Freer, R. A. Alden, S. L. Edwards, U. Skogland, K. Takio, B. Eriksson, N. H. Xuong, T. Yonetani, J. Kraut, *J. Biol. Chem.* **1980**, *255*, 575 – 580; d) G. V. Louie, W. L. B. Hutcheon, G. D. Brayer, *J. Mol. Biol.* **1988**, *199*, 295 – 314; e) S. Northrup, J. Boles, J. Reynolds, *Science* **1988**, *241*, 67 – 70.

[10] a) A. N. Volkov, J. A. R. Worrall, E. Holtzmann, M. Ubbink, *Proc. Natl. Acad. Sci. USA* **2006**, *103*, 18945 – 18950; b) Q. Bashir, A. N. Volkov, G. M. Ullmann, M. Ubbink, *J. Am. Chem. Soc.* **2010**, *132*, 241 – 247.

[11] A. N. Volkov, Q. Bashir, J. A. R. Worrall, G. M. Ullmann, M. Ubbink, *J. Am. Chem. Soc.* **2010**, *132*, 11487 – 11495.

[12] L. Geren, S. Hahm, B. Durham, F. Millett, *Biochemistry* **1991**, *30*, 9450 – 9457.

[13] J. A. R. Worrall, U. Kolczak, G. W. Canters, M. Ubbink, *Biochemistry* **2001**, *40*, 7069 – 7076.

[14] M. A. Miller, R. Q. Liu, S. Hahm, L. Geren, S. Hibdon, J. Kraut, B. Durham, F. Millett, *Biochemistry* **1994**, *33*, 8686 – 8693.

[15] a) J. E. Erman, L. B. Vitello, N. M. Pearl, T. Jacobson, M. Francis, E. Alberts, A. Kou, K. Bujarska, *Biochemistry* **2015**, *54*, 4845 – 4854; b) N. M. Pearl, T. Jacobson, M. Arisa, L. B. Vitello, J. E. Erman, *Biochemistry* **2007**, *46*, 8263 – 8272; c) N. M. Pearl, T. Jacobson, C. Meyen, A. G. Clementz, E. Y. Ok, E. Choi, K. Wilson, L. B. Vitello, J. E. Erman, *Biochemistry* **2008**, *47*, 2766 – 2775.

[16] W. Humphrey, A. Dalke, K. Schulten, *J. Mol. Graph.* **1996**, *14*, 33 – 38.

[17] G. Castro, C. A. Boswell, S. H. Northrup, *J. Biomol. Struct. Dyn.* **1998**, *16*, 413 – 424.

[18] a) J. A. R. Worrall, Y. J. Liu, P. B. Crowley, J. M. Nocek, B. M. Hoffman, M. Ubbink, *Biochemistry* **2002**, *41*, 11721 – 11730; b) J. A. R. Worrall, W. Reinle, R. Bernhardt, M. Ubbink, *Biochemistry* **2003**, *42*, 7068 – 7076; c) X. F. Xu, W. G. Reinle, F. Hannemann, P. V. Konarev, D. I. Svergun, R. Bernhardt, M. Ubbink, *J. Am. Chem. Soc.* **2008**, *130*, 6395 – 6403.

[19] a) G. M. Clore, J. Iwahara, *Chem. Rev.* **2009**, *109*, 4108 – 4139; b) G. Otting in *Annual Review of Biophysics*, *Vol. 39* (Eds.: D. C. Rees, K. A. Dill, J. R. Williamson), Annual Reviews, Palo Alto, **2010**, p. 387.

[20] A. N. Volkov, M. Ubbink, N. A. J. van Nuland, *J. Biomol. NMR* **2010**, *48*, 225 – 236.

[21] a) J. E. Erman, L. B. Vitello, J. M. Mauro, J. Kraut, *Biochemistry* **1989**, *28*, 7992 – 7995; b) C. P. Scholes, Y. J. Liu, L. A. Fishel, M. F. Farnum, J. M. Mauro, J. Kraut, *Isr. J. Chem.* **1989**, *29*, 85 – 92; c) M. Sivaraja, D. B. Goodin, M. Smith, B. M. Hoffman, *Science* **1989**, *245*, 738 – 740.

[22] a) A. F. W. Coulson, J. E. Erman, T. Yonetani, *J. Biol. Chem.* **1971**, *246*, 917 – 924; b) F. E. Summers, J. E. Erman, *J. Biol. Chem.* **1988**, *263*, 14267 – 14275.

[23] a) A. L. Matthis, J. E. Erman, *Biochemistry* **1995**, *34*, 9985 – 9990; b) A. L. Matthis, L. B. Vitello, J. E. Erman, *Biochemistry* **1995**, *34*, 9991 – 9999; c) J. S. Zhou, B. M. Hoffman, *Science* **1994**, *265*, 1693 – 1696; d) K. Van de Water, Y. G. J. Sterckx, A. N. Volkov, *Nat. Commun.* **2015**, *6*, 7073; e) G. McLendon, Q. Zhang, S. A. Wallin, R. M. Miller, V. Billstone, K. G. Spears, B. M. Hoffman, *J. Am. Chem. Soc.* **1993**, *115*, 3665 – 3669.

[24] J. M. Foerster, I. Poehner, G. M. Ullmann, *ACS Omega* **2018**, *3*, 6465 – 6475.

Manuscript received: July 21, 2020
Accepted manuscript online: August 22, 2020
Version of record online: October 13, 2020

 © 2020 The Authors. Published by Wiley-VCH GmbH